Enhancing the detectivity of an upconversion single-photon detector by spatial filtering of upconverted parametric fluorescence

Meng, Lichun; Høgstedt, Lasse; Tidemand-Lichtenberg, Peter; Pedersen, Christian; Rodrigo, Peter John

Published in:
Optics Express

Link to article, DOI:
10.1364/OE.26.024712

Publication date:
2018

Document Version
Publisher's PDF, also known as Version of record

Research Article | Vol. 26, No. 19 | 17 Sep 2018 | OPTICS EXPRESS 24712
Optics EXPRESS

Enhancing the detectivity of an upconversion single-photon detector by spatial filtering of upconverted parametric fluorescence

LICHUN MENG,[1] LASSE HØGSTEDT,[2] PETER TIDEMAND-LICHTENBERG,[1] CHRISTIAN PEDERSEN,[1] AND PETER JOHN RODRIGO[1,*]

[1]DTU Fotonik, Department of Photonics Engineering, Technical University of Denmark, Frederiksborgvej 399, 4000 Roskilde, Denmark
[2]NLIR ApS, Hirsemarken 1, 3520 Farum, Denmark
*pejr@fotonik.dtu.dk

Abstract: Due to advantages of low dark-count rate, reduced dead-time, and room-temperature operation, single-photon upconversion detectors for the telecom band are gaining strong interest as an alternative to other single-photon counters. In this work, we investigate the spatial and spectral distribution of upconverted spontaneous parametric downconversion (USPDC) noise, which is the typical dominant noise source in short-wavelength-pumped single-photon upconversion detectors for 1.5 μm – 1.6 μm. Our upconversion detector relies on a bulk periodically poled lithium niobate (PPLN) crystal and a 1064 nm intracavity pump system that spectrally translates the signal to the visible (~630 nm) where efficient, uncooled, and low dark-count Si based single-photon detectors operate. Experimental results show that the spectral and spatial distribution of the USPDC noise has a relatively broadband and radially modulated pattern that depends on the PPLN temperature, which is in good agreement with our numerical simulations. We also demonstrate that for narrow-linewidth 1575 nm signal photons, the dark-count rate can be significantly reduced by (1) using a phase-matched signal angle that corresponds to an upconverted output angle where the USPDC noise is at a "local minimum" and (2) applying a spatial filter (instead of an ultra-narrow bandpass filter) at the output. This simple spatial filtering technique resulted in a 14 dB dark-count rate reduction. Due to a corresponding decrease in the interaction length of the signal with the pump, the upconversion efficiency also decreased, but only with a 2.2 dB penalty.

1. Introduction

Frequency upconversion is a promising technology for infrared (IR) detection, and it has already been demonstrated in applications such as hyperspectral imaging [1], gas sensing [2] and single-photon counting [3–5]. Instead of measuring an IR signal directly, it is first mixed with a high-intensity pump field in a second-order nonlinear crystal and upconverted into a signal at the visible or near-IR range, which can then be detected by high-performance silicon or InGaAs based detector. In general, an upconversion detector (UCD) achieves higher detectivity and shorter response time at room temperature operation in comparison to conventional semiconductor based IR detectors. For single-photon counting, an UCD can compete with superconducting single-photon detectors but the need for a cryogenic cooling system is circumvented. The specific UCD design varies depending on the application, but high-intensity pump field (usually obtained by either a pulsed laser or an intracavity enhanced cw laser) is required in order to achieve high upconversion efficiency. However, a high-intensity pump field in the nonlinear material usually leads to some unwanted parametric processes, which can induce noise photons within the acceptance bandwidth of the UCD. One well-known example is the upconverted spontaneous parametric downconversion (USPDC) noise generated in the poled nonlinear crystal when a short-wavelength pump (i.e., the

#340742 https://doi.org/10.1364/OE.26.024712
Journal © 2018 Received 25 Jul 2018; accepted 1 Sep 2018; published 6 Sep 2018

Optics EXPRESS

wavelength of the pump is shorter than that of the signal) is used by the UCD, and its typical dark-count rate (DCR) can be 5×10^5 count/s at 1.5 μm [6]. In some particular applications, the USPDC noise can be suppressed by using a long-wavelength pump, which can lower the DCR down to ~10^3 count/s that mainly originates from spontaneous Raman scattering [7,8]. However, long-wavelength pumping has some challenges for upconversion detection in the mid-IR or far-IR range. The two main reasons are: (1) it is impractical to build a high-power pump laser in the mid-IR or far-IR range; (2) the upconverted signal in long-wavelength-pumped UCD may end up outside the sensitive spectral region of the Si/InGaAs detector. Moreover, an ultra-narrow bandpass filter such as a volume Bragg grating (VBG) may be required for DCR reduction [9].

In this paper, we report the first experimental and theoretical study of the spatial and spectral distribution of the USPDC noise when a short-wavelength pump is applied in an upconversion single-photon detector. A new physical model considering the non-collinear parametric process is developed in order to explain our experimental observations. Furthermore, we propose a novel yet simple method of using a spatial filter for DCR reduction by taking advantage of the spatially non-uniform intensity distribution and the relatively broadband spectrum of the noise. We present an experimental demonstration showing 14 dB DCR reduction with only a 2.2 dB penalty for the signal.

2. Spatial distribution of upconverted SPDC noise

The unique spatial distribution of the USPDC noise was first observed when the background noise of the intracavity pumped upconverter was measured by a very sensitive electron multiplying CCD (EM-CCD) camera that has single-photon counting capability. We believe this is a newly discovered phenomena that can be exploited for DCR suppression in upconversion detectors. Therefore, further experimental and theoretical investigations were performed.

2.1 Experiment

Figure 1 shows the experimental setup where the ring pattern of USPDC noise from a short-wavelength-pumped UCD was first discovered. More details of the UCD can be found in our previous work [10]. It is worth mentioning that the USPDC noise locates in the transmission window of the bandpass (BP) filter set in front of the EM-CCD camera (Luca S 658M, Andor). Three images of the ring pattern as shown in Fig. 1 were obtained using three different periodically poled lithium niobate (PPLN) crystals at the same operating temperature T = 50 °C. PPLN 1 has a length of 25 mm and a poling period of $\Lambda = 11.97$ μm. PPLN 2 and PPLN 3 are both 40 mm long with $\Lambda = 12$ μm. All three PPLN crystals have a lateral size of 1 mm x 1 mm. The ring patterns from these three crystals are different from each other. This suggests that it is the specific poling structure rather than the design parameters of each crystal that determines the distribution of the ring pattern. Additionally, the output of a 633 nm He-Ne laser was transmitted through the PPLN directly and no interference ring pattern was found. Thus, interference was ruled out as a mechanism for the ring pattern generation.

Optics EXPRESS

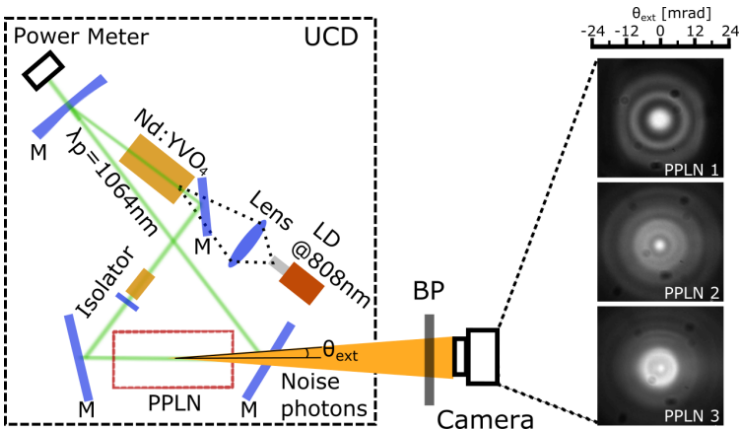

Fig. 1. Experimental setup for the USPDC ring pattern observation and three images taken by the camera for three different PPLN crystals at the same operating temperature T = 50 °C. M, mirrors; LD, laser diode. The BP filter set contain a 600 nm long-pass filter, a 650 nm short-pass filter, and a bandpass filter with a central wavelength of 635 nm and a FWHM = 10 nm. The scale on top of the images indicates the angle θ_{ext} corresponding to a lateral position on the image. Diffraction patterns caused by dust particles on the filter are visible on the image.

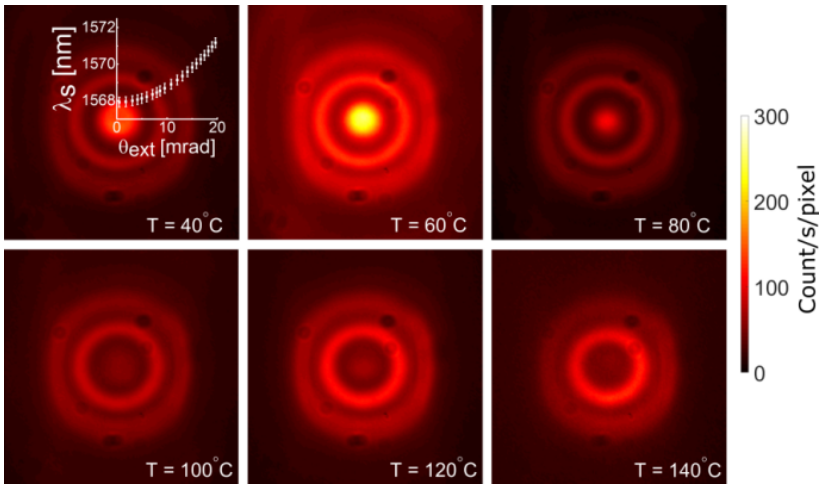

Fig. 2. Intensity profiles of the USPDC noise for PPLN 1 crystal operating at different temperatures (see Visualization 1).

Figure 2 shows the USPDC ring pattern of PPLN 1 crystal operating at different temperatures. The diameter of the rings decreased with increasing temperature. The overlay plot with the ring pattern at T = 40 °C is calculated based on the non-collinear quasi-phase matching (QPM) condition and it shows the central wavelength λ_s of the signal as a function of the angle θ_{ext} described in Fig. 1. The length of the vertical bars included in the plot indicates the acceptance bandwidth ($\Delta\lambda_s \approx 0.52$ nm). The spectral content of the ring pattern at different position varies along the radius. The average intensity of the ring pattern is also found to vary with temperature. We primarily attribute the temperature-dependence of the average intensity of USPDC to the variation of the 1064 nm pump power inside the laser cavity with changing PPLN temperature.

2.2 Theory

Due to present restrictions in the manufacturing technique, random-duty-cycle (RDC) error in QPM devices (e.g. PPLN crystal) is unavoidable. It leads to the pedestal effect that triggers USPDC photon generation when a short-wavelength pump is applied in a UCD [11]. Previous theoretical treatment of USPDC generation [11] mainly focuses on the intensity calculation

Optics EXPRESS

with collinear interaction. In order to explain the angular distribution of USPDC noise photons that was observed in the experiment, a model involving the non-collinear interaction needs to be established.

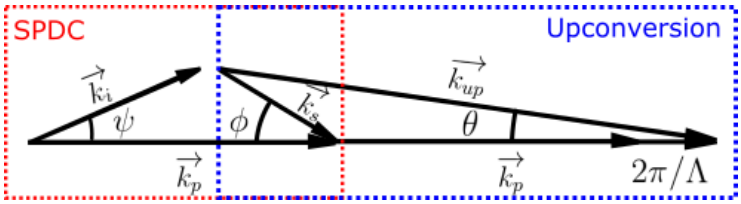

Fig. 3. k-vectors for the phase mismatched but parasitic SPDC process (red dotted region) followed by the quasi-phase-matched upconversion process (blue dotted region).

Figure 3 shows the non-collinear parametric process that is described in our proposed model. The poling period is Λ, $k_j = 2\pi n_j/\lambda_j$ is the wave vector and subscripts *i, s, p* and *up* represent the idler, signal, pump and the upconversion fields, respectively. n_j is the refractive index and λ_j is the wavelength. Using the assumption of non-collinear plane wave interaction with small angles, non-depleted pump, and transverse momentum conservation, the electric field E_j propagating along the *z*-direction is governed by the differential equations [12]

$$\begin{aligned}
\frac{dE_s}{dz} &= K_s g(z) E_i \exp(ik_d z) + K_{up} g(z) E_{up} \exp(ik_{up} z), \\
\frac{dE_i}{dz} &= K_i g(z) E_s \exp(ik_d z) \\
\frac{dE_{up}}{dz} &= K_{up} g(z) E_s \exp(ik_{up} z)
\end{aligned} \tag{1}$$

where

$$\begin{aligned}
K_j &= \frac{2i\omega_j d_{eff}}{n_j c} E_p, \quad j = s, i, \text{and } up \\
\Delta k_{up} &= k_{up}(1-\frac{\theta^2}{2}) - k_s(1-\frac{\phi^2}{2}) - k_p = k_{up} - k_s - k_p + (k_s - \frac{k_s^2}{k_{up}})\frac{\phi^2}{2}, \\
\Delta k_d &= k_p - k_i(1-\frac{\psi^2}{2}) - k_s(1-\frac{\phi^2}{2}) = k_p - k_s - k_i + (k_s + \frac{k_s^2}{k_i})\frac{\phi^2}{2} \\
g(z) &= \begin{cases} 1 & \text{odd domain} \\ -1 & \text{even domain} \end{cases}
\end{aligned} \tag{2}$$

Δk_{up} and Δk_d are the phase mismatch of the upconversion and the downconversion, respectively. d_{eff} and $g(z)$ represent the nonlinear coefficient and the poling structure of the PPLN crystal, respectively. The maximum upconversion efficiency is expected when the non-collinear QPM condition is fulfilled, i.e.,

$$\Delta k_{up}(\lambda_s, \phi) = 2\pi / \Lambda. \tag{3}$$

2.3 Simulations

According to the length, poling period Λ and specified RDC error of PPLN 1, $g(z)$ is assigned with discrete values. Afterwards, E_s and E_{up} are solved numerically based on Eq. (1) for a given λ_s and ϕ. Figure 4 shows an example of the numerical calculation. As expected, the normally phase mismatched SPDC photons are broadband. Unlike the spectrum of the SPDC,

Optics EXPRESS

the spectral coverage of USPDC photons is narrower with the central peak governed by the non-collinear QPM condition, i.e., the quasi-phase-matched upconversion process with the condition given by Eq. (3) determines where the USPDC photon count will be significant.

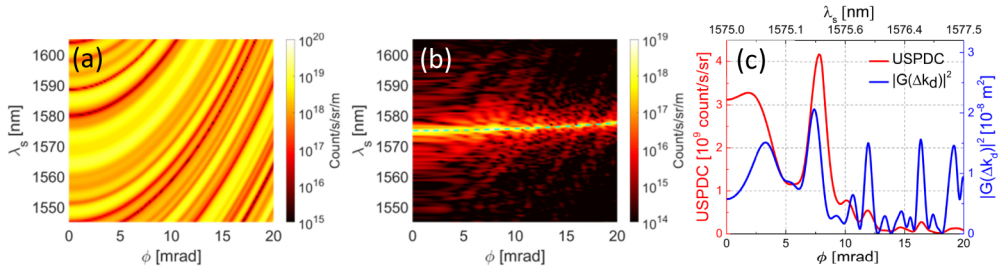

Fig. 4. (a) SPDC and (b) USPDC given by the simulation results. (c) Angular profile of the USPDC noise and the corresponding spectrum $|G(\Delta k_d)|^2$ of the simulated poling structure.

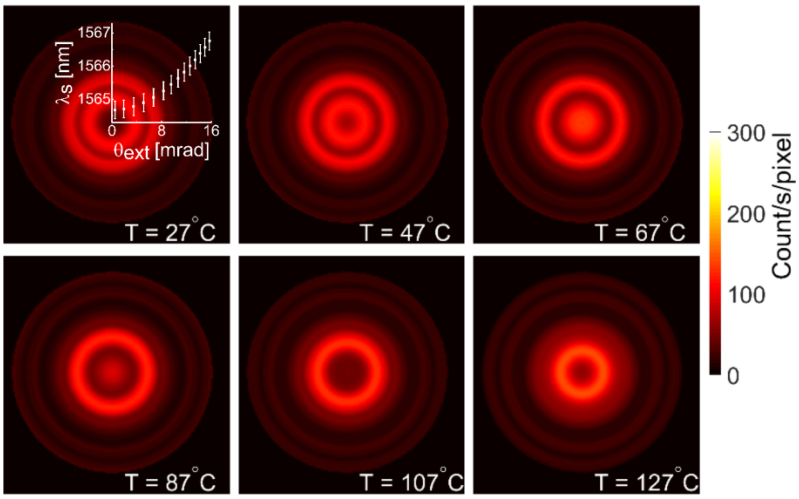

Fig. 5. Simulation results showing the USPDC pattern using crystal parameters specified for PPLN 1 operating at different temperatures considering the 45% (at 635 nm) quantum efficiency of the EM-CCD camera (see Visualization 2).

In the simulation, the following parameter settings were used: 1064 nm pump power P_p = 100 W, pump beam diameter $2\omega_0$ = 400 μm, PPLN length L = 25 mm, poling period Λ = 11.97 μm, T = 66.7 °C and the RDC error is 6% with a Gaussian distribution. The red dash curve in Fig. 4(c) is the angular profile of the USPDC photon count rate obtained by integrating Fig. 4(b) over the λ_s axis (i.e., a range that, on the upconverted side, corresponds to the 635 ± 5 nm pass-band of the filter used in the experiment), and the blue dash curve is the $|G(\Delta k_d)|^2$ [13], where $G(\Delta k_d)$ is the Fourier transform of $g(z)$, and Δk_d is given by Eq. (2) and Eq. (3). The strong correlation between these two curves indicates that the USPDC can be separated into SPDC and upconversion stages. The SPDC process is phase mismatched, but not negligible, and the profile of I_{SPDC} is decided by the specific poling structure with a corresponding $|G(\Delta k_d)|^2$. The upconversion efficiency $\eta_{up}(\lambda_s, \phi)$ has the optimum values when Eq. (3) is satisfied. Assuming that the acceptance bandwidth and angle are small enough ($\Delta\lambda_s$ < 1 nm, $\Delta\phi \sim 1$ mrad), the upconversion efficiency can be simplified as $\eta_{up}(\lambda_s, \phi) = \eta(\phi)\delta(\Delta k_{up} - 2\pi/\Lambda)$, where $\eta(\phi)$ is the upconversion efficiency considering the reduction of interaction length due to the non-collinear interaction [14]. Then, the power of USPDC can be written as:

Optics EXPRESS

$$P_{USPDC}(\theta) \propto \int I_{SPDC}(\lambda_s, \phi) \cdot \eta_{up}(\lambda_s, \phi) d\lambda_s$$
$$= \int I_{SPDC}(\lambda_s, \phi) \cdot \eta(\phi) \delta(\Delta k_{up} - 2\pi / \Lambda) d\lambda_s . \quad (4)$$
$$= \eta(\phi) I_{SPDC}(\Delta k_{up} = 2\pi / \Lambda, \phi)$$

Thus, the angular profile of the USPDC power is mainly decided by the SPDC intensity profile combined with the quasi-phase matched upconversion process.

By converting the angular distribution of the USPDC noise into a radial profile, the two-dimensional USPDC pattern with rotation symmetry was generated. Figure 5 shows the USPDC pattern with the same simulation parameters except for the crystal temperature. Consistent with the experimental result, the simulated USPDC noise emerges as a ring pattern; the diameter of the ring decreases with increasing temperature and that the radial positions of local minima change with temperature.

3. Signal-to-noise ratio improvement for short-wavelength-pumped upconversion single-photon detector

When a monochromatic IR signal is measured with the UCD, the bandwidth of the upconverted signal is usually narrower than that of the USPDC noise. Therefore, the use of a narrow bandpass (spectral) filter was the typical method for DCR reduction in previous works [15,16]. Our experiments and simulations showed that both the intensity and the spectrum of USPDC noise vary spatially, which implies that the noise can also be removed by spatial filtering when the upconverted signal is located at a local minimum of the noise pattern. A demonstration of weak IR signal detection, at low photon count rates measurable with single-photon counters, was performed in order to confirm this novel DCR reduction scheme.

3.1 Experimental setup

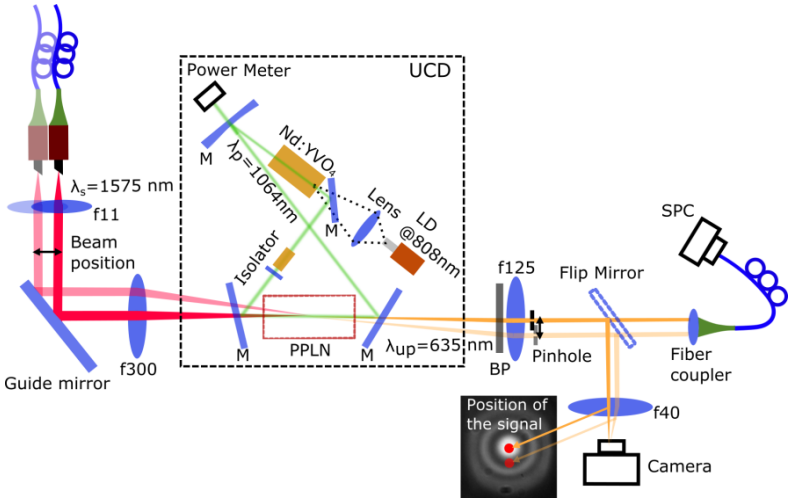

Fig. 6. Experimental setup for single-photon detection based on short-wavelength-pumped UCD. SPC, single-photon counter (Si based); LD, laser diode; BP, bandpass filter set.

Figure 6 shows a setup for single-photon detection with a short-wavelength-pumped UCD. The linearly polarized output of a fiber laser at 1575 nm was attenuated to the pW level before coupling into the UCD. The fiber tip and the collimating lens were mounted onto a translation stage, which enabled angle tuning of the IR signal by translating the stage horizontally. The IR signal was mixed with the 1064 nm pump field inside a 25 mm long PPLN crystal with Λ = 11.97 μm. The power of the upconversion signal was optimized by tuning the angle of incidence of the IR signal for different operating temperatures of the

Optics EXPRESS

PPLN crystal. After collimation and spatial filtering, the upconverter output was guided by a flip mirror, and either measured by a Si based single-photon counter (COUNT-250C-FC, intrinsic DCR = 70 s^{-1}, Laser Components) directly or imaged by a camera. The red dots on the USPDC ring pattern in Fig. 6 illustrate two different positions of the upconverted signal for two different angles ϕ. Using the collinear case (ϕ = 0), the efficiencies of different components used in the experiment were characterized as shown in Table 1.

Table 1. Efficiency characterization

Mirror transmission	Internal upconversion efficiency η_{up}	Pinhole efficiency	Fiber coupling efficiency	QE of SPC @635nm	Total efficiency η_{tot}
72%	6%	83%	81%	73%	2.1%

The diameter of the pinhole in Fig. 6 was 400 μm, which corresponded to the width of the innermost dark annular region of the USPDC noise pattern shown in the inset of Fig. 6. Therefore, a strongly reduced DCR was expected when the pinhole was placed at the local minimum of the noise pattern. Meanwhile, in order to ensure that the upconverted signal passed through the pinhole efficiently, the IR signal from the single mode fiber (N.A. = 0.12; mode-field diameter = 10 μm) was coupled inside the PPLN with a 4f lens system (f300 and f11 with focal length of 300 mm and 11 mm, respectively). The diameter of the upconverted signal at the position of the pinhole (placed after a collimating lens f125 with focal length of 125 mm) was around 450 μm, which was comparable to the size of the pinhole. However, the $1/e^2$ beam diameter of the IR signal inside the PPLN crystal was ~270 μm, which is larger than the required value that leads to optimal spatial overlap between the interacting pump and IR signal. Therefore, the measured internal upconversion efficiency η_{up} (6%) was lower than the theoretical one (16%) considering a 60 W 1064 nm pump power with a pump size $2\omega_0$ = 400 μm. In principle, we can further improve η_{up} by increasing the pump power. Using a similar UCD design (Λ = 12.07 μm, λ_s = 1646 nm), we have previously demonstrated that a 160 W pump with optimal spatial overlap with the signal can achieve η_{up} as high as 45% [2]. In this work, a moderate pump power was used to maintain a stable operation of the UCD over the range of operating temperature in which USPDC noise was investigated.

3.2 Results

For every PPLN crystal operating temperature, the IR signal angle ϕ was fine tuned in order to maximize the power of the upconverted signal. The red square in Fig. 7(a) shows the temperature of the PPLN crystal versus the experimentally obtained optimal ϕ, along with the numerical result (black curve) given by the QPM condition. The upconverted signal count rate (SCR) and the DCR are shown in Figs. 7(b) and 7(c), respectively. The collinear upconversion was achieved at 68.5 °C. The markers A and B indicate the data for cases with and without pinhole, respectively. Comparing these two cases, the SCR and DCR were reduced by 0.6 dB and 8 dB, respectively. With increasing angle ϕ, the SCR decreased due to a reduction in the effective crystal length [14]. Comparing the collinear upconversion (marker A) at 68.5 °C with the non-collinear case at 66.4 °C (marker C), the DCR decreased from ~1.4×10^4 s^{-1} to ~3.6×10^3 s^{-1} with a signal reduction of 1.6 dB.

Optics EXPRESS

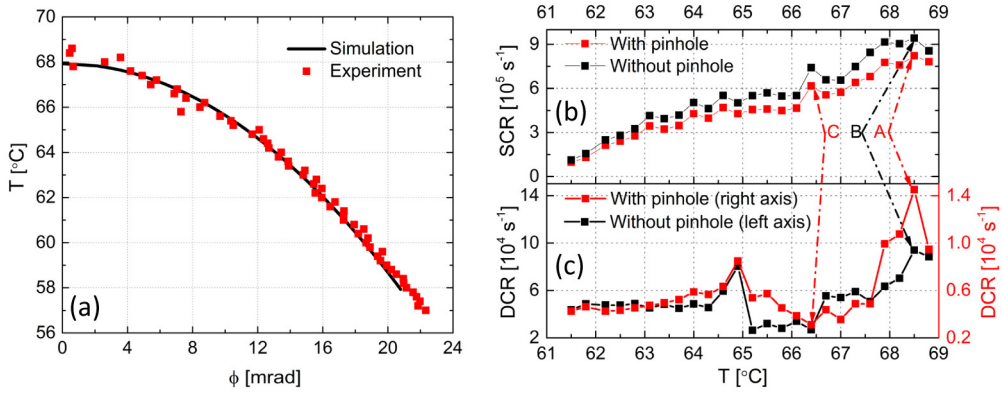

Fig. 7. (a) PPLN crystal temperature versus the corresponding optimal IR signal angle ϕ. The red square is the experimental result and the black curve is the numerical simulation given by the QPM condition. Due to slight discrepancy introduced by the Sellmeier equations, a small offset of 1.2 °C is used in the simulated results in order to fit with the experimental one. (b) SCR and (c) DCR measured at different operating temperatures of the PPLN crystal.

Comparing the collinear upconversion without pinhole (marker B) to the non-collinear case with the spatial filter at the local minimum (marker C), our method achieved a DCR reduction of 14 dB with only a 2.2 dB penalty on the SCR. Based on the formula for the noise-equivalent-power (*NEP*) calculation [17]:

$$NEP = \hbar\omega_s \sqrt{2DCR} / \eta_{tot} \tag{5}$$

The *NEP* values at marker B and C are around 2.2 fW/Hz$^{1/2}$ and 0.7 fW/Hz$^{1/2}$, respectively. Therefore, our proposed method achieved an overall *NEP* improvement factor of 3.

At marker B, the measured DCR is ~1 × 10^5 s^{-1}. Using the same parameters as the simulation result shown in Fig. 4, the USPDC count rate of 22 virtual PPLN crystals with the same RDC error of 6% but different poling structures were calculated. The average USPDC count rate is 3.0 × 10^5 s^{-1} (standard deviation of 1.3 × 10^5 s^{-1}), which is in the same order of magnitude as the measured DCR.

Based on both our experimental and theoretical investigations, the USPDC photons are mainly distributed in a solid cone corresponding to –15 mrad < θ_{ext} < 15 mrad and the spectrum of the noise pattern at different position varies along the radius. Therefore, the central wavelength of the spatially filtered noise is determined by the pinhole position on the USPDC noise pattern. Furthermore, the diameter of the pinhole and the acceptance bandwidth of the upconversion process determine the final spectral bandwidth of the noise. For example, Fig. 8(a) shows the USPDC pattern at a PPLN crystal temperature T = 65 °C. A pinhole with a diameter of 400 μm located at θ_{ext} = 6 mrad (local minimum between the central peak and the innermost bright ring) would result in λ_s = 1574.8 nm and $\Delta\lambda_s$ = 0.5 nm. Figure 8(b) is for the case of T = 140 °C, in which the local minimum locates near the center of the ring pattern. A larger pinhole can be applied in this case since the dark area around the local minimum is larger than in the previous one. Therefore, using collinear upconversion that maximizes interaction length (and, thus, conversion efficiency), a centered pinhole of 1.2 mm diameter would result in λ_s = 1597.5 nm and $\Delta\lambda_s$ = 0.6 nm. A larger pinhole also means that the IR signal can be focused with a beam diameter of less than 270 μm inside the PPLN crystal to optimize its spatial overlap with the pump beam and consequently improve conversion efficiency. The bandwidth of the upconverted noise after the pinhole is $\Delta\lambda_{up} = \Delta\lambda_s \lambda^2_{up}/\lambda^2_s$ = 0.1 nm, which is comparable to the 0.06 nm bandwidth of the VBG used in a previous work on DCR reduction with a spectral filter [9].

Optics EXPRESS

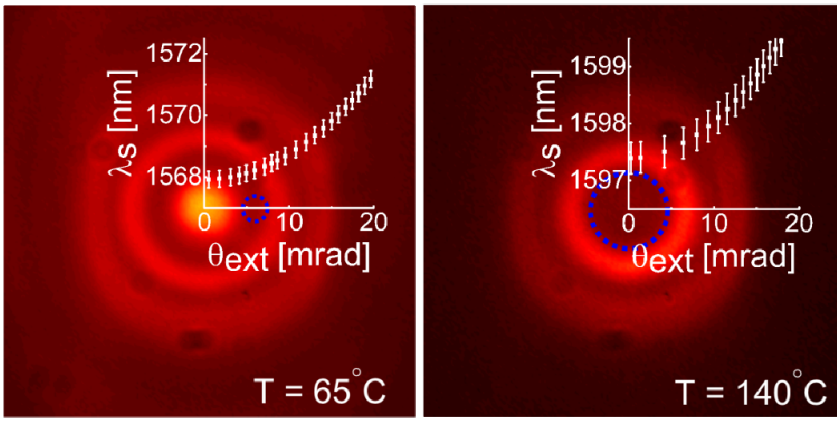

Fig. 8. USPDC pattern for PPLN 1 operating at temperature of 65 °C and 140 °C. The overlay plots show λ_s as a function of θ_{ext}. The blue dash circles indicate the areas from which to collect the upconverted signal.

For weak IR signal detection with short-wavelength-pumped UCD, the procedure for noise reduction with a pinhole is summarized as follows: First, optimize the collinear conversion efficiency by temperature tuning and obtain the corresponding USPDC noise pattern. Second, locate the local minimum of the noise pattern and choose a pinhole with the proper size that matches the width of the darkest annular region of the noise pattern. Third, with the assistance of a sensitive (EM-CCD) camera, fine tune the temperature of the PPLN crystal until the upconversion signal locates at a local minimum of the noise pattern. Fourth, block the noise with the pinhole and measure the upconverted signal with a Si based single-photon counter.

4. Summary and Discussion

For the first time, the non-uniform angular distribution of USPDC noise photons was measured in a short-wavelength-pumped UCD based on a bulk PPLN crystal. In order to explain its mechanism, a model considering non-collinear parametric interaction was established. Due to the presence of RDC error in the PPLN crystal poling structure, the SPDC intensity is enhanced, and it also has a unique spatial and spectral distribution $I_{SPDC}(\lambda_s, \phi)$. However, only the SPDC photons that fulfill the non-collinear QPM condition $\Delta k_{up}(\lambda_s, \phi) = 2\pi/\Lambda$ can be further upconverted efficiently. Therefore, the intensity of USPDC noise can be written as a function of the IR signal angle ϕ only. In order to further verify our model, simulations were run, and the results were consistent with the experimental results: (1) the USPDC photons given by simulation results also have angular distribution in both spatial and spectral region of interest. The USPDC count rate given by the simulation is comparable to the experimental one. (2) The rings in the spatial pattern of USPDC photons given by both experimental and numerical results contract towards the center with the increase of temperature. (3) The PPLN crystal with the same designed parameters but different RDC error shows different ring patterns.

Based on the discovery of the USPDC ring pattern, we proposed a simple method for DCR reduction in single-photon detection using UCD. By choosing the proper non-collinear upconversion, the position of the upconverted signal can be moved to a local minimum of the USPDC ring pattern that enables a more efficient spatial filtering of the USPDC noise. Accordingly, a single-photon detection experiment based on the short-wavelength-pumped UCD was performed. Our method achieved a 14 dB DCR reduction with only 2.2 dB penalty in SCR.

The central wavelength of the filtered USPDC noise photons is a function of the radial position of the pinhole on the ring pattern, and the 400 μm diameter pinhole used in our

Optics EXPRESS

experiment is equivalent to an ultra-narrow (spectral) bandpass filter with a FWHM of ~0.1 nm at the output of the upconverter. Therefore, our method is a promising alternative to the use of expensive bandpass filters (e.g. volume Bragg grating). Moreover, the pinhole used in the experiment can be replaced by an annular aperture for free-space IR signal detection considering a ring-shaped upconverted signal. In our previous work where UCD was used for an atmospheric Lidar application [2], no spatial filter was applied for USPDC noise reduction. If an annular aperture is applied in that experiment, the signal-to-noise ratio of the detector is expected to improve following the same principle of using a pinhole to suppress USPDC noise without significant signal losses as demonstrated in this paper. The use of a spatial filter is also a potential low-cost alternative to the use of ultra-narrow bandpass filters to reduce the DCR in 2 μm upconversion detector (with 1064 nm pump) [18] and in long-wavelength-pumped UCDs based on bulk periodically poled nonlinear crystals (i.e., suppression of upconverted spontaneous Raman scattering noise).

The side-effect of using non-collinear upconversion for DCR reduction is the decrease in total detection efficiency. However, our experiment also showed that a local minimum could also appear in the center of the ring pattern where collinear upconversion occurs. This implies that for a certain IR wavelength signal, maximum detection efficiency and significant DCR reduction by simple spatial filtering can be achieved simultaneously.

Funding

Mid-TECH – H2020-MSCA-ITN-2014 (642661).

References

1. L. M. Kehlet, P. Tidemand-Lichtenberg, J. S. Dam, and C. Pedersen, "Infrared upconversion hyperspectral imaging," Opt. Lett. **40**(6), 938–941 (2015).
2. L. Meng, A. Fix, M. Wirth, L. Høgstedt, P. Tidemand-Lichtenberg, C. Pedersen, and P. J. Rodrigo, "Upconversion detector for range-resolved DIAL measurement of atmospheric CH_4," Opt. Express **26**(4), 3850–3860 (2018).
3. J. S. Dam, P. Tidemand-Lichtenberg, and C. Pedersen, "Room-temperature mid-infrared single-photon spectral imaging," Nat. Photonics **6**(11), 788–793 (2012).
4. A. P. Vandevender and P. G. Kwiat, "High efficiency single photon detection via frequency up-conversion," J. Mod. Opt. **51**(9-10), 1433–1445 (2004).
5. L. Ma, O. Slattery, and X. Tang, "Single photon frequency up-conversion and its applications," Phys. Rep. **521**(2), 69–94 (2012).
6. M. A. Albota and F. N. Wong, "Efficient single-photon counting at 1.55 μm by means of frequency upconversion," Opt. Lett. **29**(13), 1449–1451 (2004).
7. J. S. Pelc, L. Ma, C. R. Phillips, Q. Zhang, C. Langrock, O. Slattery, X. Tang, and M. M. Fejer, "Long-wavelength-pumped upconversion single-photon detector at 1550 nm: performance and noise analysis," Opt. Express **19**(22), 21445–21456 (2011).
8. P. S. Kuo, J. S. Pelc, C. Langrock, and M. M. Fejer, "Using temperature to reduce noise in quantum frequency conversion," Opt. Lett. **43**(9), 2034–2037 (2018).
9. P. S. Kuo, J. S. Pelc, O. Slattery, Y.-S. Kim, M. M. Fejer, and X. Tang, "Reducing noise in single-photon-level frequency conversion," Opt. Lett. **38**(8), 1310–1312 (2013).
10. L. Meng, L. Høgstedt, P. Tidemand-Lichtenberg, C. Pedersen, and P. J. Rodrigo, "GHz-bandwidth upconversion detector using a unidirectional ring cavity to reduce multilongitudinal mode pump effects," Opt. Express **25**(13), 14783–14794 (2017).
11. J. S. Pelc, C. R. Phillips, D. Chang, C. Langrock, and M. M. Fejer, "Efficiency pedestal in quasi-phase-matching devices with random duty-cycle errors," Opt. Lett. **36**(6), 864–866 (2011).
12. R. W. Boyd, *Nonlinear Optics* (Academic Press, 2003).
13. C. Phillips, J. Pelc, and M. Fejer, "Parametric processes in quasi-phasematching gratings with random duty cycle errors," J. Opt. Soc. Am. B **30**(4), 982–993 (2013).
14. S. Wolf, J. Kiessling, M. Kunz, G. Popko, K. Buse, and F. Kühnemann, "Upconversion-enabled array spectrometer for the mid-infrared, featuring kilohertz spectra acquisition rates," Opt. Express **25**(13), 14504–14515 (2017).
15. M. A. Albota and F. N. C. Wong, "Efficient single-photon counting at 1.55 μm by means of frequency upconversion," Opt. Lett. **29**(13), 1449–1451 (2004).
16. H. Pan and H. Zeng, "Efficient and stable single-photon counting at 1.55 μm by intracavity frequency upconversion," Opt. Lett. **31**(6), 793–795 (2006).

Optics EXPRESS

17. A. Korneev, V. Matvienko, O. Minaeva, I. Milostnaya, I. Rubtsova, G. Chulkova, K. Smirnov, V. Voronov, G. Goltsman, W. Slysz, A. Pearlman, A. Verevkin, and R. Sobolewski, "Quantum Efficiency and Noise Equivalent Power of Nanostructured, NbN, Single-Photon Detectors in the Wavelength Range From Visible to Infrared," IEEE Trans. Appl. Supercond. **15**(2), 571–574 (2005).
18. T. Wong, J. Yu, Y. Bai, W. Johnson, S. Chen, M. Petros, and U. N. Singh, "Sensitive infrared signal detection by upconversion technique," Opt. Eng. **53**(10), 107102 (2014).